1 Supplementary Information to "Comparison of OH reactivity measurements in the atmospheric simulation chamber SAPHIR"

1.1 Fit procedures for LP-LIF instruments

In LP-LIF instruments the decay of OH in the presence of OH reactants is directly measured. The OH reactivity is the pseudo-first order decay time, if no significant OH production occurs on the time scale of measurement (up to 1 s) as for example at high NO concentrations above 20 ppbv (see manuscript for details).

The fit is done by a χ^2 minimization method (Levenberg-Marquardt fit). However, the exact evaluation procedures of the different LP-LIF instruments differ:

- FZJS and FZJM instruments use a weighted fit, for which either errors from averaging several decay curves are used or errors calculated from photon counting statistics (Poisson statistics). Both error estimates lead to similar results. The fit starts at a 95 % level of the maximum count rate and all data is used to the end of the measured decay (1 s).

- The decay curve measured by the Lille LP-LIF instrument is fitted by an unweighted fit procedure. The fit starts at a fixed time of 12 ms after the photolysis shot was applied. The end of the fit is variable and depends on the OH reactivity value. The fit length is limited to 15 times of the inverse OH reactivity or the maximum of the measured decay (1 s). The OH reactivity value used to determine the fit length is derived from applying this procedure twice starting with the maximum fit length.

- Also the fit procedure applied to decay curves by the Leeds LP-LIF instrument uses an unweighted fit. Typically the fit starts 5 ms after the firing of the photolysis laser and stops at the end of the measured decay curve. In this campaign, the decay was measured over 0.3 s. In order to avoid artifacts from initial spatial inhomogeneities in the OH distribution, the final OH reactivity value was determined by moving the start of the fit to later times using an iterative procedure until no significant change in the returned value of the OH reactivity. In this campaign, the fit range was adapted depending on a first estimate of the OH reactivity and the presence of NO in order to minimize effects from an initial fast decay that was observed, and which is attributed to an instrumental artifact specific to this campaign (see manuscript for details).

1.2 Correction of Lille LP-LIF measurements

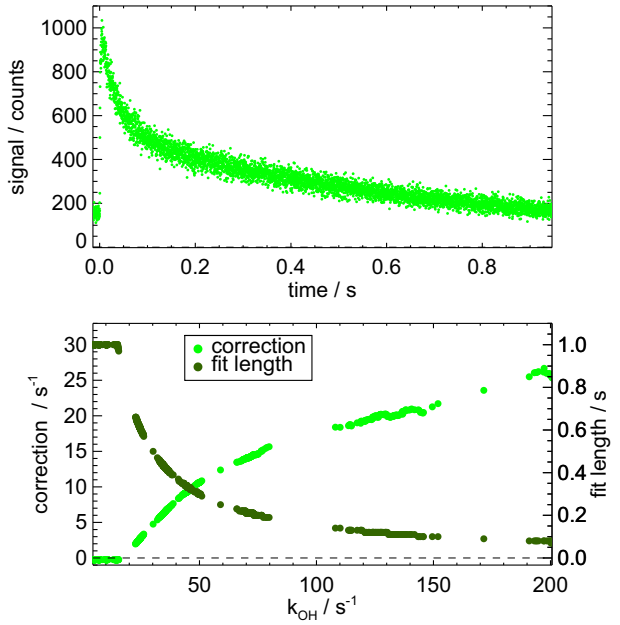

Figure 1. Example of an OH decay measurement of the Lille LP-LIF instrument obtained when sampling zero air (upper panel). The decay deviates from a single exponential behavior. Therefore, the fit result depends on the length of the fit range starting at 12 ms. For the evaluation of measurements, the fit range was dynamically changed depending on the current OH reactivity value (lower panel). Measurements were corrected by subtracting an offset value (lower panel) derived from the fit of the zero decay for the same fit range that increases with increasing OH reactivity in addition to the constant zero decay value of 4.1 s^{-1} (subtracted for the correction plotted in the lower panel).

Table 1. Summary of daily CIMS measurement values of $\ln([\mathrm{OH}]t_1/[\mathrm{OH}]t_2)$ during chamber humidification and zero OH reactivity periods at beginning of each day.

date	mean $\pm 1\sigma\,\mathrm{s}^{-1}$
07 April 2016	0.95 ± 0.03
08 April 2016	0.89 ± 0.05
09 April 2016	0.93 ± 0.06
11 April 2016	0.91 ± 0.07
12 April 2016	0.92 ± 0.02
13 April 2016	0.92 ± 0.11
14 April 2016	0.93 ± 0.07
15 April 2016	0.95 ± 0.06
all data	0.95 ± 0.03

1.3 Correction of DWD measurements

Initially CIMS OH reactivity was calculated using the values for some parameters determined during the campaign itself, with the intention to utilize all available information to create the most representative OH reactivity dataset. However this approach led to creating a dataset that was not entirely independent to the OH reactivity values for all the experiments during the campaign, e.g. not independent on the zero OH reactivity measurements at the beginning of each day. In the first submitted dataset, the zero decay or wall loss rate k_w was based on the mean of all zero measurements ($\ln([\mathrm{OH}]t_1/[\mathrm{OH}]t_2)$, (Muller et al., 2017)) from all campaign days (periods of zero OH reactivity and chamber humidification lasting about 30 to 40 min), Table 1.

The time constant t_c (= 1/reaction time) initially used was based on the CO experiment on 07 April 2016 for which measured CO concentration in the chamber were released as part of testing instrument functionality at the beginning of the campaign. The time constant was calculated for OH reactivity from 0 to $20\,\mathrm{s}^{-1}$, using the IUPAC rate constant recommendation for the reaction of CO with OH reactions (Atkinson et al., 2006).This CO-based time constant was 8.81 ± 0.08.

To produce a CIMS OH reactivity dataset that is strictly independent of measurements made at the chamber, it was decided to use the parameters of time constant and wall loss rate determined in an OH reactivity calibration experiment carried out prior to the campaign on 06 April 2016, using propane as OH reactant a bottled zero air (Linde, purity 99.999 %) (see Muller et al. (2017) for experiment description). This produced a time constant of $8.37 \pm 0.25\,\mathrm{s}^{-1}$, a zero OH reactivity value of $\ln([\mathrm{OH}]t_1/[\mathrm{OH}]t_2) = 0.99\,\mathrm{s}^{-1}$, and consequently a wall loss rate of $k_w = 8.28 \pm 0.24\mathrm{s}^{-1}$. These are the parameter values used in the final submitted dataset presented in this paper.

Taking this approach is reasonable as during long-term operation at the Meteorological Observatory Hohenpeissenberg, the zero is also not measured every day, but rather periodically and then applied over the given period of time, assuming stability of the instrument. Applying the independent and different time constant and wall loss parameter values meant that all initially submitted data changed, allowing e.g. for the bias in zero to be compared (Table 5, Figure 5). In summary, based on that change, CIMS OH reactivity is on average 10 % lower than in the first submitted dataset.

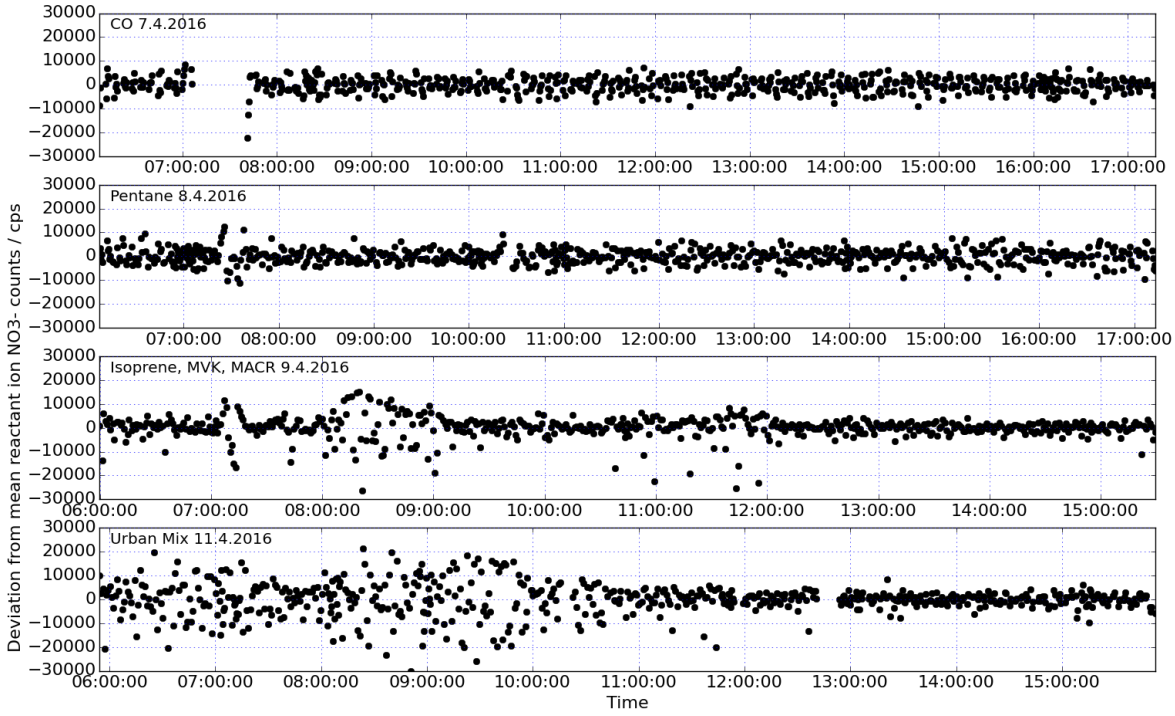

Figure 2. DWD-CIMS reactant ion (NO_3^-) residuals from running mean NO_3^- counts for experimental days 07 to 11 April 2016, illustrating higher noise and instability on 09 and 11 April 2016.

1.4 Underestimation of DWD-CIMS OH reactivity and water vapor effect on 09 and 11 April 2016: reactant ion counts

The reason for the large discrepancy and underestimation of DWD-CIMS measurements on e.g. 09 and 11 April 2016 at higher OH reactivity was investigated and no unequivocal cause could be found. However, higher noise in the CIMS reactant ion counts (NO_3^-) coincided with these periods.

Figure 2 shows the noise in the reactant ions counts in the DWD-CIMS instrument during the first four days of the 2016 campaign. On both 07 and 08 April 2016, the noise in the reactant ion counts was stable and OH reactivity measurements (Fig. 3 in the paper) do not exhibit irregular features. However CIMS OH reactivity between 08:00 to 09:00 on 09 April displayed large noise and underestimation, which is coincident with more noise in the reactant ion counts for the same time frame (Fig. 2). OH reactivity does not show the same scatter in the afternoon hours for the second injection of isoprene, MVK and MACR and noise in the reactant ions is equally reduced. A similar picture is apparent for the experiment on 11 April 2016. In the morning hours till 11:00, the NO_3^- ion noise is greatly increased. The afternoon hours show low levels of noise, which corresponds to a better agreement of CIMS OH reactivity with results from FZJS instrument. Whilst inexplicable that such a first injection-second injection /morning-afternoon "split" should exist, it is noted that a better level of agreement in OH reactivity corresponds to periods with lower noise in NO_3^- reactant ion counts. Noise levels were increased but mostly stable throughout the experiments for the rest of the campaign (not shown here). The exact reason why there was an increase in noise in reactant ion concentrations remains unclear. The system seemed to be between "two states" which would imply a

particular condition affected the instrument, producing this phenomenon. However, no technical error or clear explanation was unequivocally found, which would warrant flagging the data as invalid.

It is also noteworthy that during the periods of water vapor addition on both mornings of 09 and 11 April 2016, CIMS OH reactivity deviates from the trend of the reference OH reactivity. This response to the humidification of the chamber was not seen during most other periods of water vapor addition and this marked effect seen on 09 and 11 April 2016 coincides with the periods of increased noise in NO_3^- reactant ion counts described above.

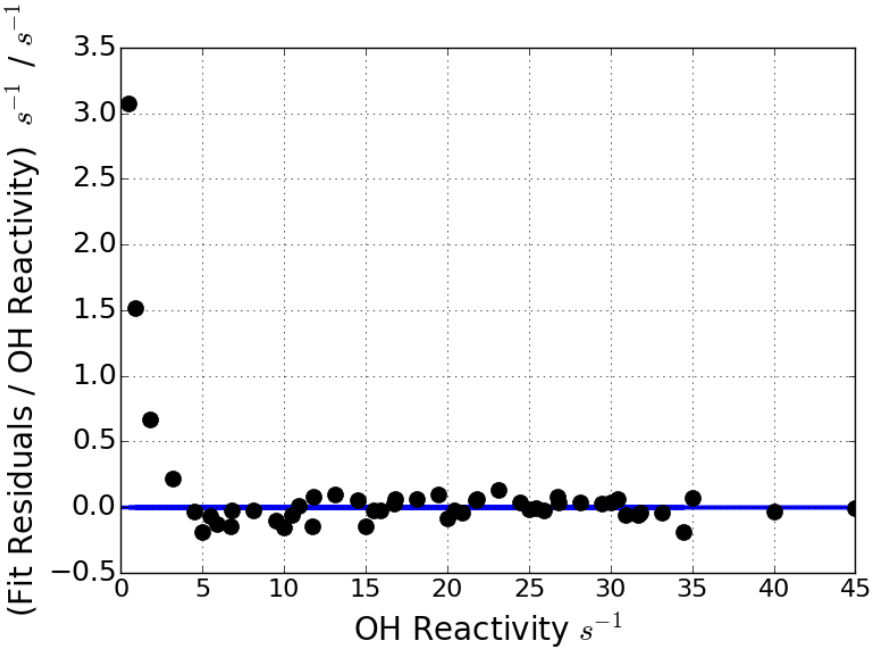

Figure 3. CIMS NO correction residuals from fitted, i.e. corrected OH reactivity and calculated OH reactivity, normalized by calculated OH reactivity, based on propane, isoprene and ethene laboratory characterization experiments, showing the quality of the fit function is systematically low below $2.5\,\mathrm{s}^{-1}$.

1.5 NO correction of DWD CIMS measurements for low reactivity values

The NO correction function was determined for OH reactivity up to $40\,\mathrm{s}^{-1}$ and NO concentrations up to 15 ppbv, which produced a good fit for OH reactivity above $2.5\,\mathrm{s}^{-1}$, but provided a systematic overestimation above that value, as seen in Fig. 3. Therefore the NO correction was not applied for OH reactivity above $2.5\,\mathrm{s}^{-1}$.

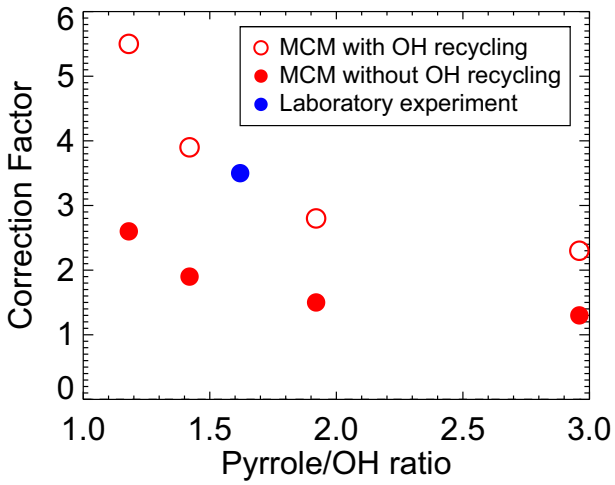

Figure 4. Comparison of simulated and measured (correction factors required to correct the CRM measurements for not operating the instrument under pseudo first order conditions. Correction factors are shown as a function of the pyrrole-to-OH ratio. Simulations were performed with and without OH recycling from the reaction of the acyl peroxy radical and HO_2.

1.6 Influence of acetaldehyde on the MDOUAI CRM measurements

The oxidation of aldehyde species by OH proceeds by H-atom abstraction from the aldehydic group, leading to the formation of acyl peroxy radicals, $RC(O)O_2$. For instance, the oxidation of acetaldehyde will lead to the formation of the acetyl peroxy radical, $CH_3C(O)O_2$, with a yield of approximately 95 % as reported by Cameron et al. (2002) and Butkovskaya et al. (2004). The reaction of acyl peroxy radicals with HO_2 is known to efficiently recycle OH in the atmosphere. For the acetyl peroxy radical, Dillon and Crowley (2008) recently reported an OH yield of 0.5. This recycling mechanism can act as a secondary source of OH in CRM instruments, which in turn can mask a fraction of the OH-reactivity from aldehyde species for these instruments, leading to a negative bias.

The impact of this chemistry on CRM measurements was investigated for the operating conditions of the Mines Douai instrument using the modeling methodology described in Michoud et al. (2015). The simulations were performed using a subset of the Master Chemical Mechanism v3.2 (http: //mcm.leeds.ac.uk/MCM), including the oxidation chemistry of acetaldehyde. The model was run using operating conditions reported by Michoud et al. (2015), which were similar to that used during the comparison campaign, and several acetaldehyde concentrations ranging from 7 to 400 ppbv, which are equivalent to OH reactivities of 2.7 to 152 s^{-1}. Figure 4 reports the correction (filled circles) that would need to be applied to the CRM measurements for not operating the instrument under pseudo first order conditions if the oxidation of acetaldehyde was not recycling OH. For these simulations the OH yield was set at zero. As shown in this figure, the correction depends on the pyrrole-to-OH ratio (C1-C2 modulation), which ranged from 1.7 to 2.2 for the Mines Douai instrument during the comparison campaign. Adding the recycling of OH with a yield of 0.5 leads to an increase of the required correction (empty circles) by approximately a factor of 2 for the range of pyrrole-to-OH ratios mentioned above. This change in the correction indicates an underestimation of the OH reactivity from acetaldehyde by a factor of 2.

An experiment was conducted by supplying a diluted mixture of acetaldehyde (112 ppbv) to the Mines Douai CRM instrument. This experiment is shown by the blue circle in Fig. 4. This result seems to confirm that the OH reactivity of acetaldehyde is underestimated by the Mines Douai instrument, which is consistent with that observed for this instrument during the 16 October 2015 experiment (Fig. 2), when acetaldehyde was first introduced in SAPHIR. However, Figure 2 shows that the two other CRM instrument (LSCE and MPI) are less (or not) impacted by OH recycling from $CH_3C(O)O_2$+HO_2. These different behaviors are not well understood and need more investigations.

1.7 Measurements in zero air

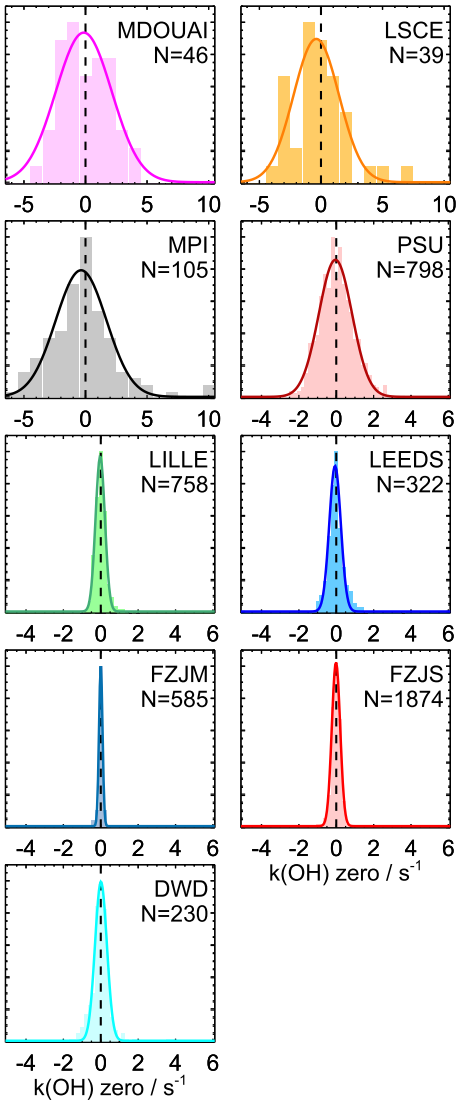

Figure 5. Distribution (bars) of OH reactivity measurements for times before OH reactants were injected into the chamber. Mean values are subtracted for individual experiments for each instrument, before combining all data in order to remove day-to-day variability of potential biases in the measurements. MDOUAI, LSCE and MPI measurements are binned to 1 s^{-1} intervals, other measurements to 0.1 s^{-1} intervals. Solid lines shows the fit to a Gaussian distribution.

1.8 Measurements in the presence of CO and/or CH_4: all data

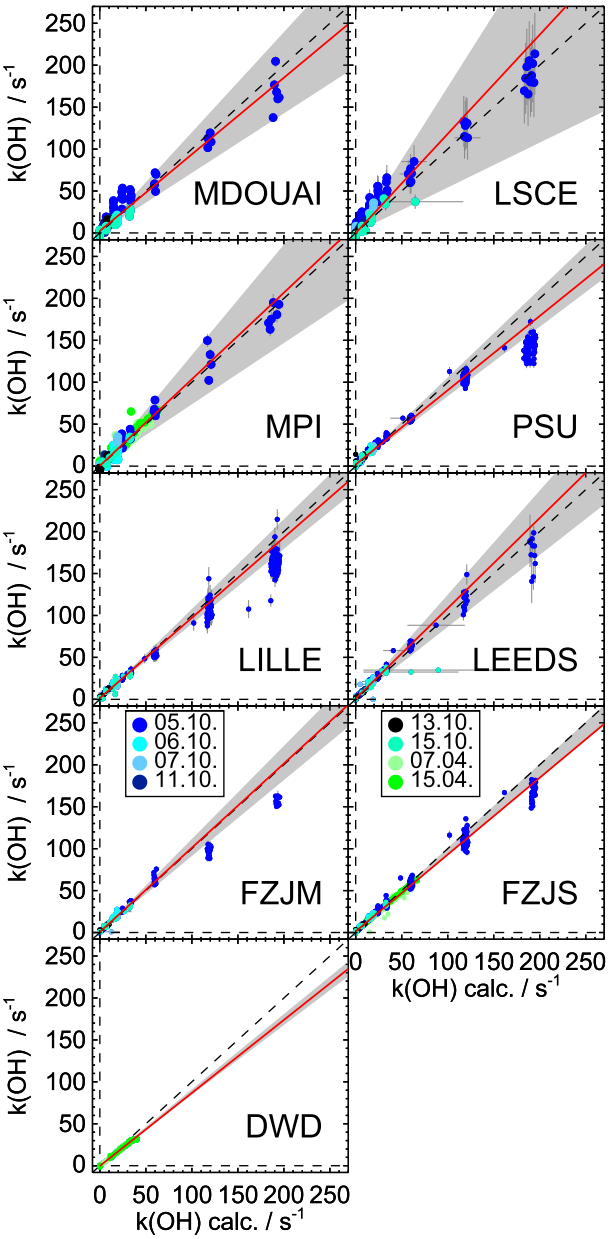

Figure 6. Correlation between measured and calculated OH reactivity for experiments in the SAPHIR chamber, if only CO, CH_4, O_3 and water vapor were present. Red lines give results of a linear regression analysis. The grey area indicates the mean relative difference between measurements and the regression line. Measurements of the MDOUAI instrument during the first three experiments (05, 06 and 07 October 2015) have a higher uncertainty due to technical problems.

Table 2. Results of the correlation analysis (linear correlation coefficient R^2 and slope and intercept of linear fit) for all data with CO, CH_4 data. Errors of fit results (not shown here) are not significant within two digits of the fit parameters. $\langle|\Delta k|/k_{fit}\rangle$ gives the mean value of the relative difference between measurements and the regression line.

data subset	instrument	# data points	R^2	slope	intercept / s^{-1}	$\langle\|\Delta k\|/k_{fit}\rangle$
CO,CH_4 [a] [b]	MDOUAI	134	0.95	0.91	2.4	0.30
	LSCE	132	0.96	1.18	-0.1	0.47
	MPI	192	0.97	1.03	0.4	0.28
	PSU	1291	0.98	0.89	2.0	0.18 [c]
	Lille	1667	0.99	0.96	1.5	0.11
	Leeds	867	0.98	1.05	1.3	0.11
	FZJM	830	0.98	1.00	0.7	0.10
	FZJS	2389	0.99	0.92	1.4	0.09
	DWD	295	0.99	0.87	-0.3	0.04

[a] 05/06/07/11/13/15 October 2015; 07/15 April 2016
[b] reference: calculated reactivity
[c] scatter amplified by the dilution factor of 5 in this campaign

1.9 Influence of water vapor in the 2015 campaign

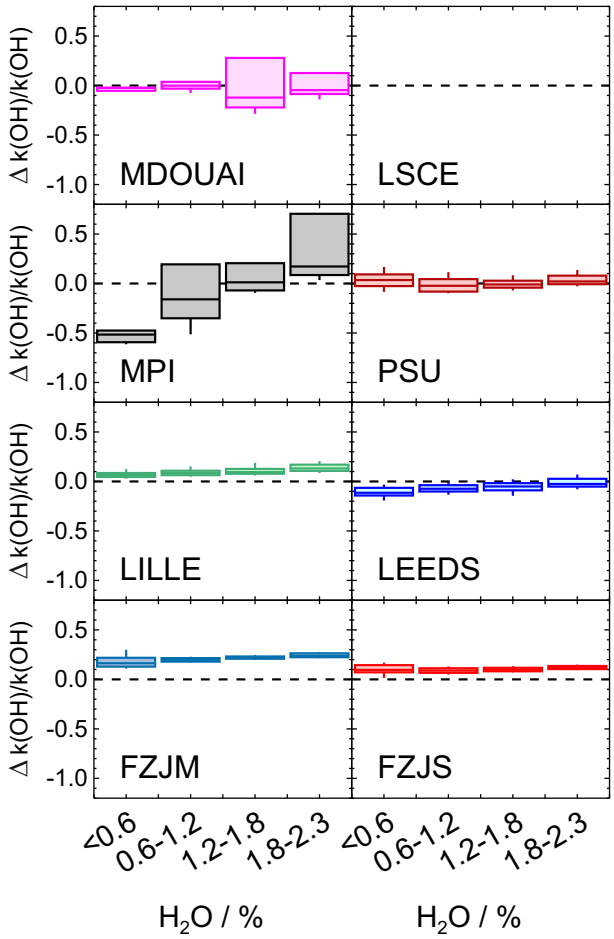

Figure 7. Relative difference between measured and calculated OH reactivity depending on the H_2O mixing ratio in the experiment on 06 October 2015. Boxes give median and 25 and 75 percentiles, whiskers give 10 and 90 percentiles. The small change in the relative difference observed for some LP-LIF instruments is within the uncertainty of the calculation using the CO concentration measurement. For the MPI CRM instrument, the change in the ratio of pyrrole to OH concentration with changing water vapor concentration might have led to systematic errors in this experiment, because the correction factor for deviations from pseudo-first order kinetics were not well characterized for low OH concentrations experienced at low water vapor concentration. No measurements were made by the LSCE-CRM instrument on that day due to technical problems.

References

Atkinson, R., Baulch, D. L., Cox, R. A., Crowley, J. N., Hampson, R. F., Hynes, R. G., Jenkin, M. E., Rossi, M. J., Troe, J., and Subcommittee, I.: Evaluated kinetic and photochemical data for atmospheric chemistry: Volume II - gas phase reactions of organic species, Atmos. Chem. Phys., 6, 3625–4055, doi:10.5194/acp-6-3625-2006, 2006.

Butkovskaya, N. I., Kukui, A., and Le Bras, G.: Branching fractions for H_2O forming channels of the reaction of OH radicals with acetaldehyde, J. Phys. Chem., 108, 1160–1168, doi:10.1021/jp036740m, 2004.

Cameron, M., Sivakumaran, V., Dillon, T. J., and Crowley, J. N.: Reaction between OH and CH_3CHO Part 1. Primary product yields of CH_3 (296 K), CH_3CO (296 K), and H (237-296 K), Phys. Chem. Chem. Phys., 4, 3628–3638, doi:10.1039/B202586H, 2002.

Dillon, T. J. and Crowley, J. N.: Direct detection of OH formation in the reactions of HO_2 with $CH_3C(O)O_2$ and other substituted peroxy radicals, Atmos. Chem. Phys., 8, 4877–4889, doi:10.5194/acp-8-4877-2008, 2008.

Michoud, V., Hansen, R. F., Locoge, N., Stevens, P. S., and Dusanter, S.: Detailed characterizations of the new Mines Douai comparative reactivity method instrument via laboratory experiments and modeling, Atmos. Meas. Tech., 8, 3537–3553, doi:10.5194/amt-8-3537-2015, 2015.

Muller, J. B. A., Kubistin, D., Elste, T., and Plaß Dülmer, C.: A novel semi-direct method to measure OH reactivity by chemical ionisation mass spectrometry (CIMS): in prep., Atmos. Meas. Tech. Discuss., 2017.